Chapter 1

Design Methodology for a Quick and Low-Cost Wind Tunnel

Miguel A. González Hernández,
Ana I. Moreno López, Artur A. Jarzabek,
José M. Perales Perales, Yuliang Wu and
Sun Xiaoxiao

Additional information is available at the end of the chapter

http://dx.doi.org/10.5772/54169

1. Introduction

Wind tunnels are devices that enable researchers to study the flow over objects of interest, the forces acting on them and their interaction with the flow, which is nowadays playing an increasingly important role due to noise pollution. Since the very first day, wind tunnels have been used to verify aerodynamic theories and facilitate the design of aircrafts and, for a very long time, this has remained their main application. Nowadays, the aerodynamic research has expanded into other fields such as automotive industry, architecture, environment, education, etc., making low speed wind tunnel tests more important. Although the usefulness of CFD methods has improved over time, thousands of hours of wind tunnel tests (WTT) are still essential for the development of a new aircraft, wind turbine or any other design that involves complex interactions with the flow. Consequently, due to the growing interest of other branches of industry and science in low speed aerodynamics, and due to the persistent incapability of achieving accurate solutions with numerical codes, low speed wind tunnels (LSWT) are essential and irreplaceable during research and design.

A crucial characteristic of wind tunnels is the flow quality inside the test chamber and the overall performances. Three main criteria that are commonly used to define them are: maximum achievable speed, flow uniformity and turbulence level. Therefore, the design aim of a wind tunnel, in general, is to get a controlled flow in the test chamber, achieving the necessary flow performance and quality parameters.

In case of the aeronautical LSWTs, the requirements of those parameters are extremely strict, often substantially increasing the cost of facilities. But low turbulence and high uniformity in the flow are only necessary when, for example, laminar boundary layers have to be investigated. Another example of their use is aircraft engines combustion testing; this in turns requires a costly system that would purify the air in the tunnel to maintain the same air quality. Another increasingly important part of aircraft design is their noise footprint and usually the only way to test this phenomenon is in a wind tunnel.

In the automotive applications, it is obvious that the aerodynamic drag of the car is of paramount importance. Nevertheless, with the currently high level of control of this parameter and also due to imposed speed limitations, most of the efforts are directed to reduce the aerodynamic noise. The ground effect simulation is also very important, resulting in very sophisticated facilities to allow testing of both the ground effect simulation and noise production in the test section.

In architecture, due to the fact that buildings are placed on the ground and are usually of relatively low height, they are well within the atmospheric boundary layer. Therefore, the simulation of the equivalent boundary layer, in terms of average speed and turbulence level, becomes a challenging problem.

The design of the wind tunnels depends mainly on their final purpose. Apart from vertical wind tunnels and others used for specific tests (e.g. pressurised or cryogenic wind tunnels), most of the LSWTs can be categorised into two basic groups: open and closed circuit. They can be further divided into open and closed test section type.

For most applications, mainly for medium and large size wind tunnels, the typical configuration is the closed circuit and closed test chamber. Although, due to the conservation of kinetic energy of the airflow, these wind tunnels achieve the highest economic operation efficiency, they prove more difficult to design resulting from their general complexity. Hence, we will pay more attention to them in this chapter.

Apart from some early built wind tunnels for educational purposes at the UPM, since 1995 a number of LSWTs have been designed following the methodology which will be presented here. It focuses on the reduction of construction and operation costs, for a given performance and quality requirements.

The design procedure was first used for a theoretical design of a LSWT for the Spanish Consejo Superior de Deportes, which was to have a test section of 3,0 x 2,5 x 10,0 m^3 with a maximum operating speed of 40 m/s. Based on this design, a 1:8 scale model was built at UPM. This scaled wind tunnel has been used for research and educational purposes.

The second time it was during the design of a LSWT for the Instituto Tecnológico y de Energías Renovables de Tenerife (ITER). That wind tunnel is in use since February 2001, operating in two configurations: medium flow quality at maximum operating speed of 57 m/s, and high flow quality at maximum operating speed of 48 m/s. For more information visit www.iter.es.

http://dx.doi.org/10.5772/54169

Another example of this design procedure is a LSWT for the Universidad Tecnológica de Perú, which is now routinely used for teaching purposes. This wind tunnel is now in operation for about one and a half year.

At the moment the same procedure is being utilised to design a LSWT for the Beijing Institute of Technology (BIT). This wind tunnel will be used for educational and research purposes. It will have a high quality flow, up to 50 m/s, in a test section of 1,4 x 1,0 x 2,0 m^3. It will be used for typical aerodynamic tests and airfoil cascade tests (utilising the first corner of the wind tunnel circuit).

The design method to be presented in this chapter is based upon classical internal ducts design and analysis method, e.g. *Memento des pertes de charge: Coefficients de pertes de charge singulières et de pertes de charge par frottement,* I.E. Idel'cik [Eyrolles, 1986]. It also includes design assisting software such as a macro-aided Excel spreadsheet with all the complete formulation and dimensioning schemes for automatic recalculation. At the moment the best example of use of the method is the BIT-LSWT, mentioned above, as it has been defined using the latest and most reliable generation of wind tunnel design methodology.

2. Main design criteria

The general layout of the proposed wind tunnel is shown in Figure 1. The airflow circulates in the direction indicated in the test chamber (counter clockwise in the figure). Upstream of the test chamber we find the other two main components of the wind tunnel: the contraction zone and the settling chamber. The other crucial component is of course the power plant. The remainder of the components just serve the purpose of closing the circuit while minimising the pressure loss. Nevertheless, diffuser 1 and corner 1 also have an important influence on the flow quality and they are responsible for more than 50% of the total pressure loss.

The design criteria are strongly linked with the specifications and requirements and those must be in accordance with the wind tunnel applications. The building and operation costs of a wind tunnel are highly related to the specifications and these are just a consequence of the expected applications.

In the case of the so called Industrial Aerodynamics or educational applications, the requirements related to flow quality may be relaxed, but for research and aeronautical applications the flow quality becomes very important, resulting in more expensive construction and higher operational costs.

The main specifications for a wind tunnel are the dimensions of the test section and the desired maximum operating speed. Together with this the flow quality, in terms of turbulence level and flow uniformity, must be specified in accordance with the applications. At this point it should also be defined whether all the components of the wind tunnel are going to be placed on the floor in a horizontal arrangement or in a vertical one, with only half of the circuit on the floor and the other half on top of it.

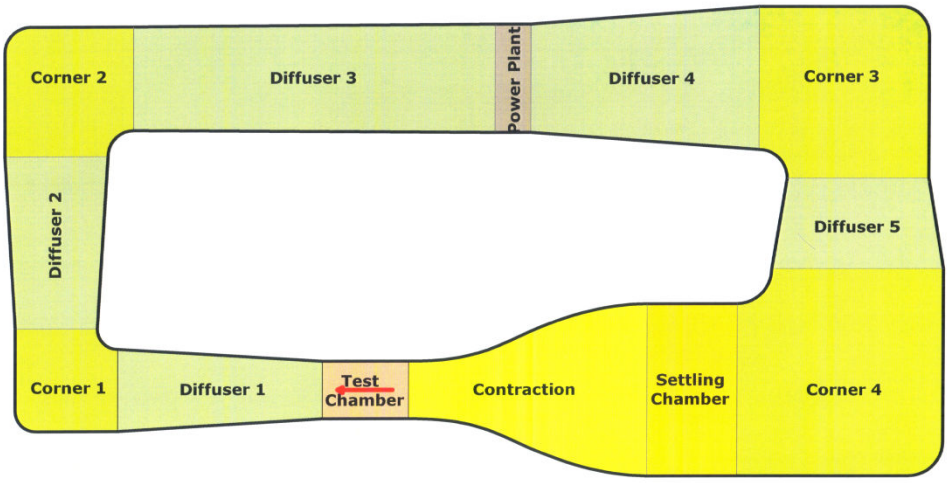

Figure 1. General layout of a closed circuit low speed wind tunnel. Figure labels indicate the part name, according to standards.

Flow quality, which is one of the main characteristics, is a result of the whole final design, and can only be verified during calibration tests. However, according to previous empirical knowledge, some rules can be followed to select adequate values of the variables that affect the associated quality parameters. The recommended values will be discussed in the sections corresponding to the Contraction, Settling Chamber, Diffusor 1 and Corner 1, which are the wind tunnel parts that have the greatest impact on the flow quality.

Once these specifications are given, it is very important to obtain on one side the overall wind tunnel dimensions to check their compatibility with the available room, and on the other side a preliminary estimation of the overall cost. The cost is mainly associated to the external shape of the wind tunnel and the power plant requirements.

For the benefit of new wind tunnel designers, a tool has been devised and implemented in an Excel spreadsheet (visit web page http://www.aero.upm.es/LSLCWT). Using this tool the designer will immediately get information about each part of the wind tunnel, the overall dimensions, the global and individual pressure loss coefficients, and the required power. This will be done according to the recommended input parameters and specification based on the intended use of the wind tunnel.

3. Wind tunnel components definition

In the following sections the design of each part will be thoroughly discussed and analysed in detail to get the best design addressing the general and particular requirements. Before dealing with each component, some general comments are given for the most important parts. In the

http://dx.doi.org/10.5772/54169

case of the contraction zone, its design is crucial for achieving the required flow quality in the test section. In this sense, its contraction ratio, length and contour definition determine the level of uniformity in the velocity profile, as well as the necessary turbulence attenuation. It is crucial to avoid flow separation close to the walls of the contraction zone. At the stage of design, the most adequate method to verify that design meets those criteria is computational fluid dynamics (CFD).

Other important parts of the wind tunnel design worth mentioning here are the corners which incorporate turning vanes. Their aim is to reduce pressure loss and, in the case of the corner 1, possibly improve flow quality in the test section. The parameters to be considered in their design are the spacing between vanes (whether the space ought to be constant or not) and the possibility of expanding the flow (increasing the cross-section).

To complete the design process, the measurement equipment needs to be defined together with the complimentary calibration tests. Special attention needs to be devoted to the specification and selection of the balance for forces measurement, a device that is used to measure aerodynamic forces and moments on the model subjected to airflow in the test section. Since the drag force on test subjects can be very small and significant noise may be coming from the vibration of the tunnel components, such as the model stand, the true drag value may become obscured. The choice of an appropriate force balance is therefore crucial in obtaining reliable and accurate measurements.

The selection depends mainly on the nature of the tests. Wind tunnel balances can be categorized into internal and external ones. The former offers mobility since it is usually only temporarily mounted to the test section and may be used in different test sections. However, the latter has more potential in terms of data accuracy and reliability since it is tailored to a specific wind tunnel and its test section. Due to this reason, external force balances should be studied in greater depth.

3.1. Test chamber

The test chamber size must be defined according to the wind tunnel main specifications, which also include the operating speed and desired flow quality. Test chamber size and operating speed determine the maximum size of the models and the maximum achievable Reynolds number.

The cross-section shape depends on the applications. In the case of civil or industrial applications, in most of the cases, a square cross-section is recommended. In this case, the test specimens are usually bluff bodies and their equivalent frontal area should not be higher than 10% of the test chamber cross-sectional area in order to avoid the need of making non-linear blockage corrections. Accurate methods for blockage corrections are presented in Maskell (1963).

Nevertheless, a rectangular shape is also recommended for aeronautical applications. In the case of three-dimensional tests, a typical width to height ratio is 4:3; however, for two-dimensional tests a 2:5 ratio is advised in order for the boundary layer thickness in the test section to be much smaller than the model span.

Taking into account that it is sometimes necessary to place additional equipment, e.g. measuring instruments, supports, etc., inside the test chamber, it is convenient to maintain the operation pressure inside it equal to the local environment pressure. To fulfil this condition, it is recommended to have a small opening, approximately 1,0% of the total length of the test chamber, at the entrance of the diffuser 1.

From the point of view of the pressure loss calculation, the test chamber will be considered as a constant section duct with standard finishing surfaces. Nevertheless, in some cases, the test chamber may have slightly divergent walls, in order to compensate for the boundary layer growth. This modification may avoid the need for tail flotation correction for aircraft model tests, although it would be strictly valid only for the design Reynolds number.

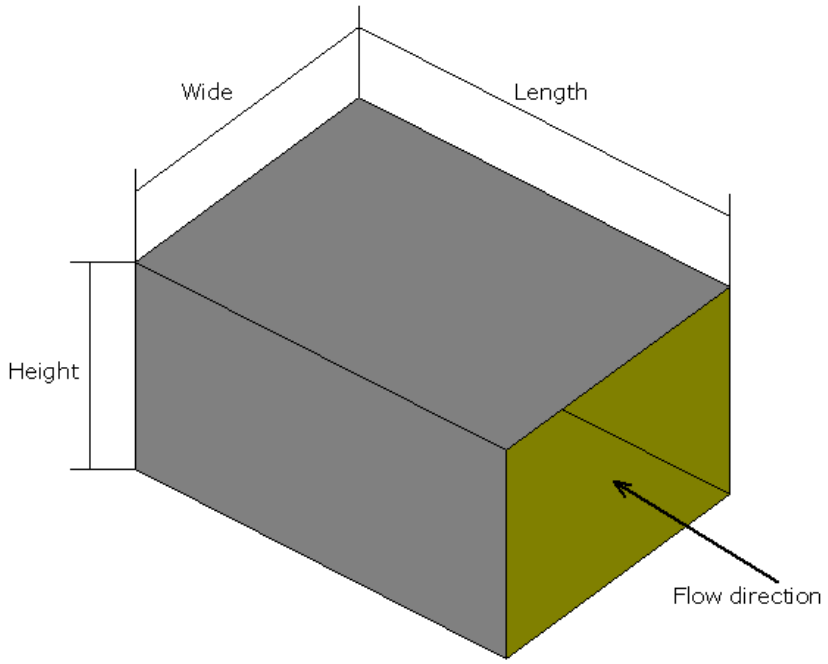

Figure 2. Layout of a constant section wind tunnel test chamber.

Figure 2 shows a design of a typical constant section test chamber. With the typical dimensions and velocities inside a wind tunnel, the flow in the test section, including the boundary layer, will be turbulent, because it is continuous along the whole wind tunnel. According to Idel´Cik (1969), the pressure loss coefficient, related to the dynamic pressure in the test section, which is considered as the reference dynamic pressure for all the calculations, is given by the expression:

$$\zeta = \lambda \cdot L \ / D_H,$$

http://dx.doi.org/10.5772/54169

where L is the length of the test chamber, D_H the hydraulic diameter and λ a coefficient given by the expression:

$$\lambda = 1 / (1{,}8 \cdot \log Re - 1{,}64)^2,$$

where Re is the Reynolds number based on the hydraulic diameter.

3.2. Contraction

The contraction or "nozzle" is the most critical part in the design of a wind tunnel; it has the highest impact on the test chamber flow quality. Its aim is to accelerate the flow from the settling chamber to the test chamber, further reducing flow turbulence and non-uniformities in the test chamber. The flow acceleration and non-uniformity attenuations mainly depend on the so-called contraction ratio, N, between the entrance and exit section areas. Figure 3 shows a typical wind tunnel contraction.

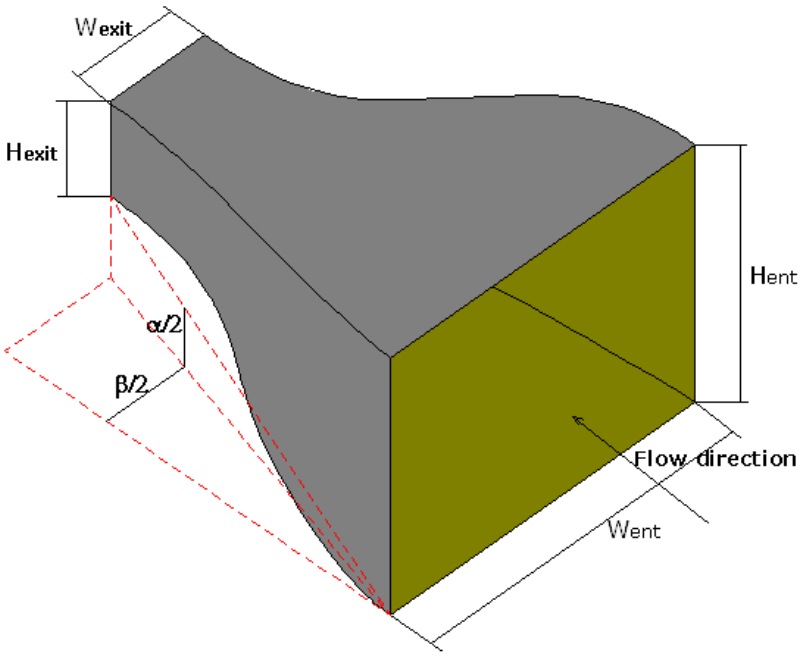

Figure 3. General layout of a three-dimensional wind tunnel contraction.

Although, due to the flow quality improvement, the contraction ratio, N, should be as large as possible, this parameter strongly influences the overall wind tunnel dimensions. Therefore, depending on the expected applications, a compromise for this parameter should be reached.

Quoting P. Bradshaw and R. Metha (1979), “The effect of a contraction on unsteady velocity variations and turbulence is more complicated: the reduction of x-component (axial) fluctuations is greater than that of transverse fluctuations. A simple analysis due to Prandtl predicts that the ratio of root-mean-square (rms) axial velocity fluctuation to mean velocity will be reduced by a factor $1/N^2$, as for mean-velocity variations, while the ratio of lateral rms fluctuations to mean velocity is reduced only by a factor of N: that is, the lateral fluctuations (in m/s, say) increase through the contraction, because of the stretching and spin-up of elementary longitudinal vortex lines. Batchelor, *The Theory of Homogeneous Turbulence*, Cambridge (1953), gives a more refined analysis, but Prandtl's results are good enough for tunnel design. The implication is that tunnel free-stream turbulence is far from isotropic. The axial-component fluctuation is easiest to measure, e.g. with a hot-wire anemometer, and is the "free-stream turbulence" value usually quoted. However, it is smaller than the others, even if it does contain a contribution from low-frequency unsteadiness of the tunnel flow as well as true turbulence.”

In the case of wind tunnels for civil or industrial applications, a contractions ratio between 4,0 and 6,0 may be sufficient. With a good design of the shape, the flow turbulence and non-uniformities levels can reach the order of 2,0%, which is acceptable for many applications. Nevertheless, with one screen placed in the settling chamber those levels can be reduced up to 0,5%, which is a very reasonable value even for some aeronautical purposes.

For more demanding aeronautical, when the flow quality must be better than 0,1% in non-uniformities of the average speed and longitudinal turbulence level, and better than 0,3% in vertical and lateral turbulence level, a contraction ratio between 8,0 and 9,0 is more desirable. This ratio also allows installing 2 or 3 screens in the settling chamber to ensure the target flow quality without high pressure losses through them.

The shape of the contraction is the second characteristic to be defined. Taking into account that the contraction is rather smooth, one may think that a one-dimensional approach to the flow analysis would be adequate to determine the pressure gradient along it. Although this is right for the average values, the pressure distribution on the contraction walls has some regions with adverse pressure gradient, which may produce local boundary layer separation. When it happens, the turbulence level increases drastically, resulting in poor flow quality in the test chamber.

According to P. Bradshaw and R. Metha (1979), “The old-style contraction shape with a small radius of curvature at the wide end and a large radius at the narrow end to provide a gentle entry to the test section is not the optimum. There is a danger of boundary-layer separation at the wide end, or perturbation of the flow through the last screen. Good practice is to make the ratio of the radius of curvature to the flow width about the same at each end. However, a too large radius of curvature at the upstream end leads to slow acceleration and therefore increased rate of growth of boundary-layer thickness, so the boundary layer - if laminar as it should be in a small tunnel - may suffer from Taylor-Goertler "centrifugal" instability when the radius of curvature decreases”.

According to our experience, when both of the contraction semi-angles, $\alpha/2$ and $\beta/2$ (see Figure 3), take the values in the order of 12º, the contraction has a reasonable length and a good fluid dynamic behaviour. With regard to the contour shape, following the recommendations of P. Bradshaw and R. Metha (1979), two segments of third degree polynomial curves are recommended.

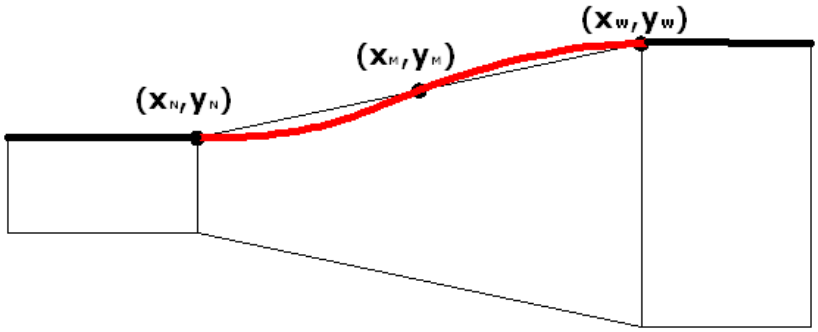

Figure 4. Fitting polynomials for contraction shape.

As indicated in Figure 4, the conditions required to define the polynomial starting at the wide end are: the coordinates (x_W,y_W), the horizontal tangential condition in that point, the point where the contour line crosses the connection strait line, usually in the 50% of such line, and the tangency with the line coming from the narrow end. For the line starting at the narrow end the initial point is (x_N,y_N), with the same horizontal tangential condition in this point, and the connection to the wide end line. Consequently, the polynomials are:

$$y = a_W + b_W \cdot x + c_W \cdot x^2 + d_W \cdot x^3,$$

$$y = a_N + b_N \cdot x + c_N \cdot x^2 + d_N \cdot x^3.$$

Imposing the condition that the connection point is in the 50%, the coordinates of that point are $[x_M,y_M]=[(x_W+x_N)/2,(y_W+y_N)/2)]$. Introducing the conditions in both polynomial equations, the two families of coefficients can be found.

According to Idel´Cik (1969), the pressure loss coefficient related to the dynamic pressure in the narrow section, is given by the expression:

$$\zeta = \left\{\frac{\lambda}{\left[16 \cdot \sin\left(\frac{\alpha}{2}\right)\right]}\right\}\left(1 - \frac{1}{N^2}\right) + \left\{\frac{\lambda}{\left[16 \cdot \sin\left(\frac{\beta}{2}\right)\right]}\right\}\left(1 - \frac{1}{N^2}\right),$$

where λ is defined as:

$$\lambda = 1 / (1{,}8 \log \mathrm{Re} - 1{,}64)^2.$$

The Reynolds number is based on the hydraulic diameter of the narrow section.

3.3. Settling chamber

Once the flow exits the fourth corner (see Figure 1), the uniformization process starts in the settling chamber. In the case of low-quality flow requirements, it is a simple constant section duct, which connects the exit of the corner 4 with the entrance of the contraction.

Nevertheless, when a high quality flow is required, some devices can be installed to increase the flow uniformity and to reduce the turbulence level at the entrance of the contraction (see Figure 5). The most commonly used devices are screens and honeycombs. Both devices achieve this goal by producing a relatively high total pressure loss; however, keeping in mind that the local dynamic pressure equals to $1/N^2$ of the reference dynamic pressure, such pressure loss will only be a small part of the overall one, assuming that N is large enough.

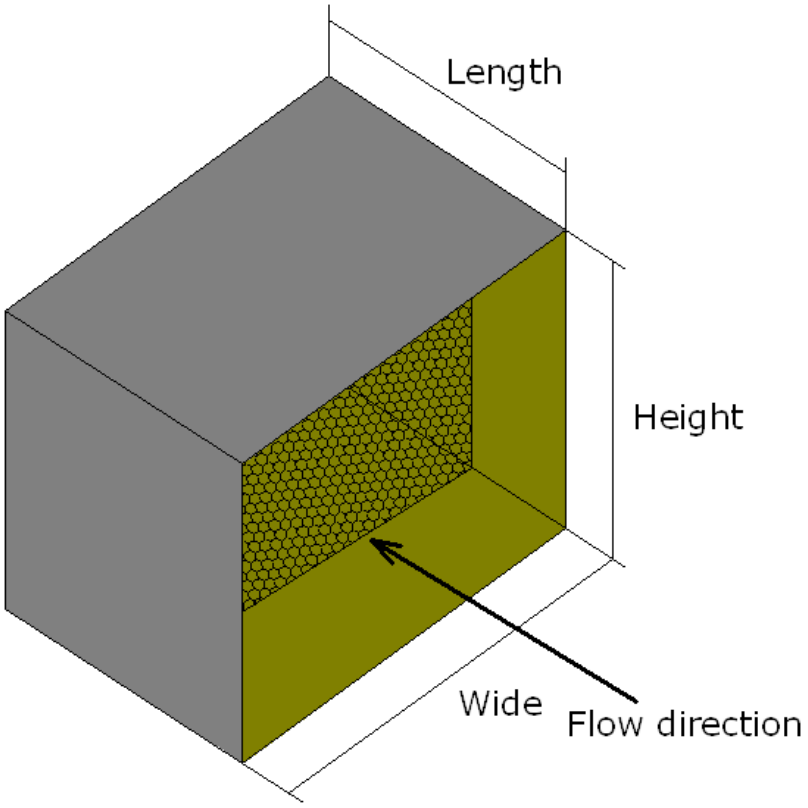

Figure 5. General layout of a settling chamber with a honeycomb layer.

Honeycomb is very efficient at reducing the lateral turbulence, as the flow pass through long and narrow pipes. Nevertheless, it introduces axial turbulence of the size equal to its diameter,

http://dx.doi.org/10.5772/54169

which restrains the thickness of the honeycomb. The length must be at least 6 times bigger than the diameter. The pressure loss coefficient, with respect to the local dynamic pressure, is about 0,50 for a 3 mm diameter and 30 mm length honeycomb at typical settling chamber velocities and corresponding Reynolds numbers.

Although screens do not significantly influence the lateral turbulence, they are very efficient at reducing the longitudinal turbulence. In this case, the problem is that in the contraction chamber the lateral turbulence is less attenuated than the longitudinal one. As mentioned above, one screen can reduce very drastically the longitudinal turbulence level; however, using a series of 2 or 3 screens can attenuate turbulence level in two directions up to the value of 0,15%. The pressure loss coefficient, with respect to the local dynamic pressure, of an 80%-porous screen made of 0,5 mm diameter wires is about 0,40.

If a better flow quality is desired, a combination of honeycomb and screens is the most recommended solution. This configuration requires the honeycomb to be located upstream of 1 or 2 screens. In this case, the pressure loss coefficient, with respect to the local dynamic pressure, is going to be about 1,5. If the contraction ratio is 9, the impact on the total pressure loss coefficient would be about 0,02, which may represents a 10% of the total pressure loss coefficient. This implies a reduction of 5% in the maximum operating speed, for a given installed power.

The values of the pressure loss coefficients given in this section are only approximated and serve as a guideline for quick design decisions. More careful calculations are recommended for the final performance analysis following Idel´Cik's (1969) methods.

3.4. Diffusers

The main function of diffusers is to recover static pressure in order to increase the wind tunnel efficiency and, of course, to close the circuit. For that reason, and some other discussed later, it is important to maintain the flow attachment for pressure recovery efficiency. Figure 6 shows the layout of a rectangular section diffuser.

Diffuser 1 pays an important role in the test chamber flow quality. In case of flow detachment, the pressure pulsation is transmitted upstream into the test chamber, resulting in pressure and velocity non-uniformities. In addition, diffuser 1 acts as a buffer in the transmission of the pressure disturbances generated in the corner 1.

It has been proved that in order to avoid flow detachment, the maximum semi-opening angle in the diffuser has to be smaller than 3,5°. On the other hand, it is important to reduce as much as possible the dynamic pressure at the entrance of the corner 1, in order to minimise the possible pressure loss. Consequently, it is strongly recommended not to exceed the semi-opening angle limit and to design the diffuser to be as long as possible.

Diffuser 2 is a transitional duct, where the dynamic pressure is still rather large. Subsequently, the design criterion imposing a maximum value of the semi-opening angle must also be applied. The length of this diffuser cannot be chosen freely, because later it becomes restrained by the geometry of corners 3 and 4 and diffuser 5.

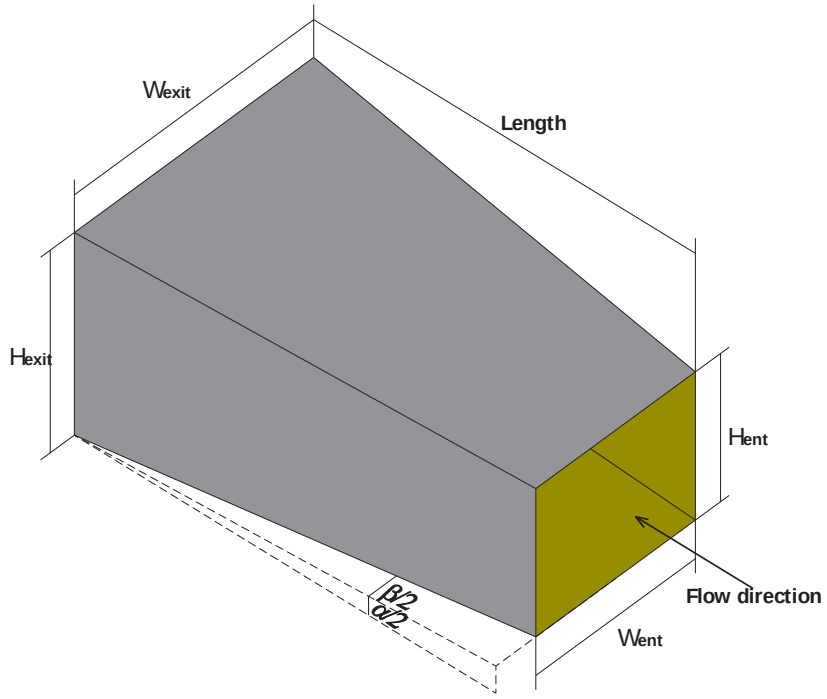

Figure 6. Rectangular section diffuser.

Diffuser 3 guides the flow to the power plant which is strongly affected by flow separation. In order to avoid it, the criterion imposing a maximum value of the semi-opening angle is maintained here as well. The cross-sectional shape may change along this diffuser because it must connect the exit of corner 2, whose shape usually resembles that of the test chamber, with the entrance of the power plant, whose shape will be discussed later.

The same can be said about diffuser 4 because pressure oscillations travel upstream and therefore may affect the power plant. Analogically to the previous case, it provides a connection between the exit of the power plant section and the corner 3, which has a cross-section shape resembling the one of the test chamber.

Diffuser 5 connects the corners 3 and 4. It is going to be very short, due to a low value of the dynamic pressure, which will allow reducing the overall wind tunnel size. This will happen mainly when the contraction ratio is high and the diffusion angle may be higher than 3,5°. It can also be used to start the adaptation between the cross-section shapes of the tests section and the power plant.

An accurate calculation of the pressure loss coefficient can be done with Idel´Cik´s (1969) method. A simplified procedure, derived from the method mentioned above, is presented here to facilitate a quick estimation of such coefficient.

http://dx.doi.org/10.5772/54169

The pressure loss coefficient, with respect to the dynamic pressure in the narrow side of the diffuser, is given by:

$$\zeta = 4{,}0 \cdot \tan\alpha / 2 \cdot \sqrt{\tan \alpha/2} \cdot \left(1 - \frac{F_0}{F_1}\right)^2 + \zeta_f .$$

α being the average opening angle, F_0 the area of the narrow section, F_1 the area of the wide section and where ζ_f is defined as:

$$\zeta_f = \frac{0{,}02}{8 \cdot \sin\alpha / 2}\left[1 - \left(\frac{F_0}{F_1}\right)^2\right].$$

3.5. Corners

Closed circuit wind tunnels require having four corners, which are responsible for more than 50% of the total pressure loss. The most critical contribution comes from the corner 1 because it introduces about 34% of the total pressure loss. To reduce the pressure loss and to improve the flow quality at the exit, corner vanes must be added. Figure 7 shows a typical wind tunnel corner, including the geometrical parameters and the positioning of corner vanes.

The width and the height at the entrance, W_{ent} and H_{ent} respectively, are given by the previous diffuser dimensions. The height at the exit, H_{exit}, should be the same as at the entrance, but the width at the exit, W_{exit}, can be increased, giving the corner an expansion ratio, W_{exit}/W_{ent}. This parameter can have positive effects on the pressure loss coefficient of values up to approximately 1,1. However, it must be designed considering specific geometrical considerations, which will be discussed, in greater details in the general arrangement.

The corner radius is another design parameter and it is normally proportional to the width at the corner entrance. The radius will be identical for the corner vanes. Although increasing the corner radius reduces the pressure loss due to the pressure distribution on corner vanes, it increases both the losses due to friction and the overall wind tunnel dimensions. According to previous experience, it is recommended to use 0,25 W_{ent} as the value of the radius for corners 1 and 2, and 0,20 W_{ent} for the other two corners.

The corner vanes spacing is another important design parameter. When the number of vanes increases, the loss due to pressure decreases, but the friction increases. Equal spacing is easier to define and sufficient for all corners apart from corner 1. In this case, in order to minimise pressure loss, the spacing should be gradually increased from the inner vanes to the outer ones.

The vanes can be defined as simple curved plates, but they can also be designed as cascade airfoils, which would lead to further pressure loss reduction. In the case of low speed wind tunnels the curved plates give reasonably good results. However, corner 1 may require to further stabilise the flow and reduce the pressure loss. Flap extensions with a length equal to the vane chord, as shown in Figure 7, is a strongly recommended solution to this problem.

Other parameters, such as the arc length of the vanes or their orientation, are beyond the scope of this chapter. For more thorough approach the reader should refer to Idel´Cik (1969), Chapter 6. As mentioned above, the pressure loss reduction in the corners is very important. Therefore,

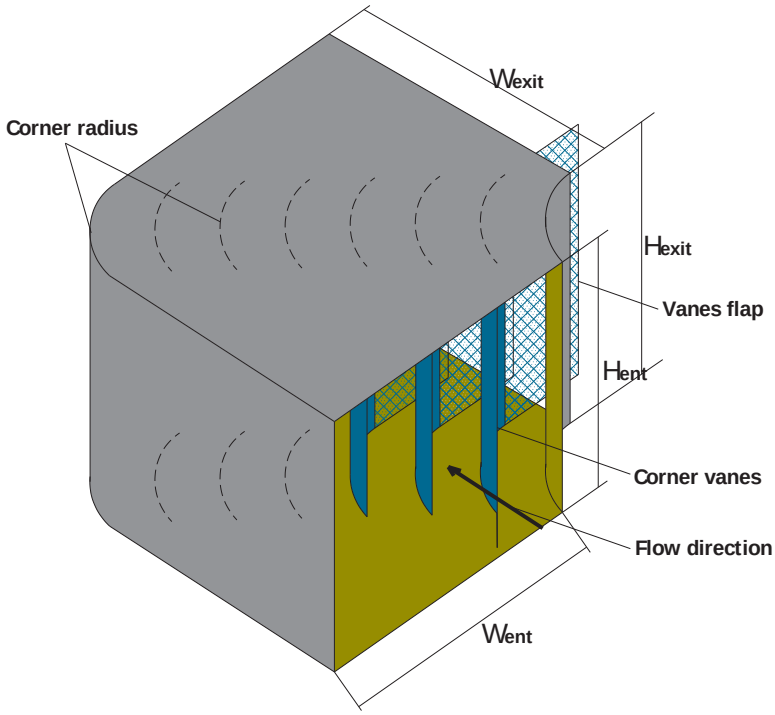

Figure 7. Scheme of a wind tunnel corner, including vanes, flaps and nomenclature.

an optimum design of these elements, at least in the case of corner 1 and 2, has a significant impact on the wind tunnel performance.

In order to allow a preliminary estimation of the pressure loss in the corners we will follow the method presented in Diagram 6.33 from Idel´Cik (1969) mentioned above. In this approach, we take an average number of vanes, $n = 1{,}4 * S/t_1$, S being the diagonal dimension of the corner, where t_1 is the chord of the vane. The pressure loss coefficient is given by the expression:

$$\zeta = \zeta_M + 0{,}02 + 0{,}031 * \frac{r}{W_{ent}}.$$

ζ_M depends on r/W_{ent}, and its values are 0,20 and 0,17 for r/W_{ent} equal to 0,20 and 0,25, respectively. As a result, the corresponding values of ζ are 0,226 and 0,198 respectively, always with respect to the dynamic pressure at the entrance. This proves the validity of the recommendations given before with regard to the value of the curvature radius and the length of diffusor 1.

3.6. Power plant

The main aim of the power plant is to maintain the flow running inside the wind tunnel at a constant speed, compensating for all the losses and dissipation. The parameters that specify it

http://dx.doi.org/10.5772/54169

are the pressure increment, Δp, the volumetric flow, Q, and the power, P. Once the test chamber cross-section surface, S_{TC}, and the desired operating speed, V, are fixed, and the total pressure loss coefficient, ζ, has been calculated, all those parameters can be calculated using:

$$\Delta p = \frac{1}{2}\rho \cdot V^2 \cdot \zeta$$

$$Q = V \cdot S_{TC}$$

$$P = \Delta p \cdot \frac{Q}{\eta},$$

where ρ is the operating air density and η the fan efficiency, accounting for both aerodynamic and electric motor efficiencies.

In order to reduce the cost of this part by roughly one order of magnitude, we propose to use a multi-ventilator matrix, as presented in Figure 8, instead of a more standard single ventilator power plant configuration. The arrangement of this matrix will be discussed later.

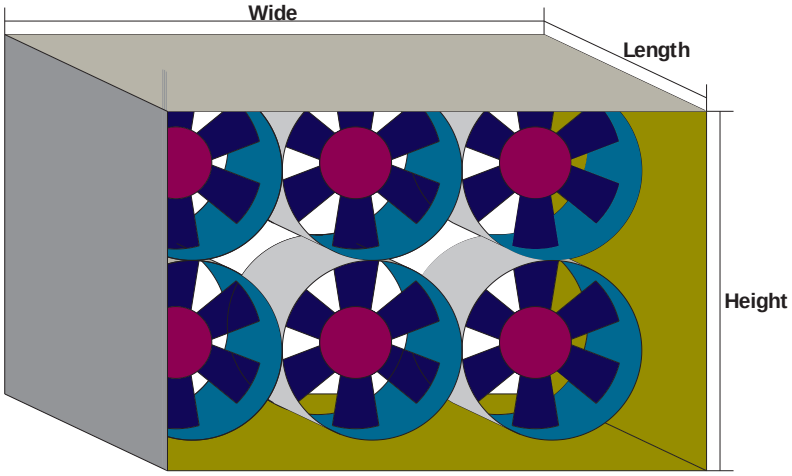

Figure 8. Layout of a multi-fan power plant.

According to our experience, for a closed circuit wind tunnel eventually including settling chamber screens or/and a honeycomb, the total pressure loss coefficient is in the range of 0,16 to 0,24. Consequently, in the case of 1,0 m^2 test section area and 80 m/s maximum operating speed, assuming an average value of ζ to be in the range mentioned above, and for a typical value of η equal to 0,65, the data specifying the power plant are:

Δp= 785 Pa, Q= 80 m^3/s, P= 100 kW.

In this case we could use a 2,0m diameter fan specially designed for this purpose or 4 commercial fans of 1,0 m diameter, producing the same pressure increment, but with a volumetric

flow of 20 m^3/s each. The latter option would reduce the total cost because the fans are a standard product.

4. General design procedure

The parameters that need to be defined in order to start the overall design are:

- Test chamber dimensions: width, W_{TC}, height, H_{TC}, and length, L_{TC}. These parameters allow to compute the cross-sectional area, $S_{TC}= W_{TC} H_{TC}$, and the hydraulic diameter, $D_{TC}=2 W_{TC} H_{TC}/(W_{TC}+ H_{TC})$.
- Contraction ratio, $N\approx5$ for low quality flow, and $N\approx9$ for high quality flow (considering the drawbacks of choosing a higher contraction ratio, explained before).
- Maximum operating speed, V_{TC}.

According to the impact on the wind tunnel dimensions and flow quality, Table 1 shows a classification of the design variables divided into two categories: main and secondary design parameters.

Main design parameters	Secondary design parameters
Maximum operating speed, V_{TC}	Contraction semi angle, $\alpha_C/2$
Test chamber width, W_{TC}	Settling chamber non-dimensional length, l_{SC}
Test chamber height, H_{TC}	Diffuser semi angle, $\alpha_D/2$
Test chamber length, L_{TC}	Diffuser 1 non-dimensional length, l_{D1}
Contraction ratio, N	Corner 1 expansion ratio, e_{C1}
	Corner 1 non-dimensional radius, r_{C1}
	Corner 4 non-dimensional radius, r_{C4}
	Diffuser 5 non-dimensional length, l_{D5}
	Corner 3 non-dimensional radius, r_{C3}
	Dimension of the fan matrix, n_W, n_H
	Unitary fan diameter, D_F
	Power plant non dimensional length, l_{PP}
	Corner 2 expansion ratio, e_{C2}

Table 1. Main and secondary wind tunnel design parameters

Now, following the guidelines given above, such as the convergence angle and the contour line shape of the contraction zone, the test and contraction chamber can be fully defined. In

http://dx.doi.org/10.5772/54169

the case when both opening angles, α and β, are the same, the contraction length, L_C, is given by the expression:

$$L_C = \frac{(\sqrt{N} - 1) \cdot W_{TC}}{2 \cdot \tan(\alpha_C / 2)}.$$

Continuing in the upstream direction, the next part to be designed is the settling chamber. The only variable to be fixed is the length, because the section is identical to the wide section of the contraction. In the case when high quality flow is required, the minimum recommended non-dimensional length based on the hydraulic diameter, l_{SC}, is 0,60. This results from the necessity to provide extra space for the honeycomb and screens. In all other cases, the non-dimensional length may be 0,50. Therefore, the length of the settling, L_{SC}, chamber is given by:

$$L_{SC} = \sqrt{N} \cdot W_{TC} \cdot l_{SC}.$$

To obtain all the data for the geometric definition of the corner 4 satisfying all the recommendations given above we only need to fix the non-dimensional radius, r_{C4}. Its length, which is the same as its width, is:

$$L_{C4} = W_{C4} = \sqrt{N} \cdot W_{TC} \cdot (1 + r_{C4}).$$

Going downstream of the test chamber, we arrive at the diffuser 1. Assuming that both semi-opening angles are 3,5°, its non-dimensional length, l_{D1}, is the only design parameter. Although it has a direct effect on the wind tunnel overall length, we must be aware that this diffuser together with corner 1 are responsible for more than 50% of the total pressure losses. According to the experience, l_{D1}>3 and l_{D1}>4 is recommended for low and high contraction ratio wind tunnels respectively. The length of the diffuser 1, L_{D1}, and the width in the wide end, W_{WD1}, is defined by:

$$L_{D1} = W_{TC} \cdot l_{D1}$$

$$W_{WD1} = [1 + 2 \cdot l_{D1} \cdot \tan(\alpha_{D1} / 2)] \cdot W_{TC}.$$

With regard to the corner 1, once its section at the entrance is fixed (it is constrained by the exit of diffuser 1), we must define the non-dimensional radius, r_{C1}, and the expansion ratio, e_{C1}. As a result, the width at the exit, W_{EC1}, the overall length, L_{C1}, and width, W_{C1}, can be calculated using:

$$W_{EC1} = W_{WD1} \cdot e_{C1}$$

$$L_{C1} = W_{WD1} \cdot (e_{C1} + r_{C1})$$

$$W_{C1} = W_{WD1} \cdot (1 + r_{C1}).$$

Therefore, we can already formulate the overall wind tunnel length, L_{WT}, as a function of the test chamber dimensions, the contraction ratio, and other secondary design parameters:

$$L_{WT} = L_{TC} + W_{TC} \cdot \left[\frac{(\sqrt{N} - 1)}{2 \cdot \tan(\alpha_C / 2)} + \sqrt{N} \cdot l_{SC} + \sqrt{N} \cdot (1 + r_{C4}) + l_{D1} + [1 + 2 \cdot l_{D1} \cdot \tan(\alpha_{D1} / 2)] \cdot (e_{C1} + r_{C1}) \right].$$

This quick calculation allows the designer to check whether the available length is sufficient to fit the wind tunnel.

Taking into account all the recommended values for the secondary design parameters, a guess value for the wind tunnel overall length, with a contraction ratio N=9 (high quality flow), is given by the formula:

$$L_{WT} = L_{TC} + 16 \cdot W_{TC}.$$

In the case when N=5 (low quality flow), the formula becomes:

$$L_{WT} = L_{TC} + 11{,}5 \cdot W_{TC}.$$

The designer must be aware that any modification introduced to the secondary design parameters modifies only slightly the factor that multiplies W_{TC} in the formulas above. Consequently, if the available space is insufficient, the only solution would be to modify the test chamber dimensions and/or the contraction ratio.

As we have already defined the wind tunnel length using the criterion of adequate flow quality, we can now devote our attention to designing the rest of the circuit, the so-called return circuit. The goal is not to increase its length, intending also to minimize the overall width and keeping the pressure loss as low as possible.

Keeping this in mind, the next step in the design is to make a first guess about the power plant dimensions. Following our design recommendations, a typical value for the total pressure loss coefficient of a low contraction ratio wind tunnel, excluding screens and honeycombs in the settling chamber, is 0,20, with respect to the dynamic pressure in the test chamber. This value is approximately 0,16 for a large contraction ratio wind tunnels. If screens and honeycombs were necessary, those figures could increase by about 20%.

As the power plant is placed more or less in the middle of the return duct, the area of the section will be similar to the mid-section of the contraction. Therefore, taking into account the volumetric flow, the total pressure loss, and the available fans, the decision about the type of fan and the number of them can be taken. Using this approach, the power plant would be defined, at least in the preliminary stage.

We will return now to the example we started before for the power plant section. To improve the understanding of the subject, we are going to present a case study. If the test chamber section was square and N=5, the mid-section of the contraction would be 1,67 x 1,67 m^2. This would allow us to place 4 standard fans of 0,800 m diameter each. The maximum reduction in the width size would be obtained by suppressing the diffuser 5, obtaining the wind tunnel platform shown in Figure 9. We have not defined the diffusion semi-angle in diffuser 3, but we checked afterwards that it was smaller than 3,5°. Figure 9 is just a wire scheme of the wind tunnel, made with an Excel spreadsheet, and for this reason the corners have not been rounded and are represented just as boxes.

In the case of a 4:3 ratio rectangular test chamber cross-section, the mid-section of the contraction would be 1,869x1,401 m^2 and for this reason we could suggest the use of 6 standard fans

http://dx.doi.org/10.5772/54169

of 0,630 m diameter, organized in a 3x2 matrix, occupying a section of 1,890x1,260 m^2. Figure 10 shows the wire scheme of this new design. We can check that the diffuser 3 semi-angle is below 3,5° as well.

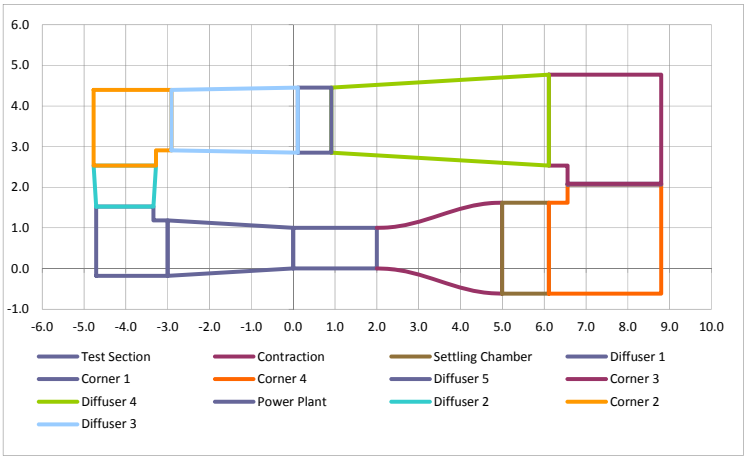

Figure 9. Non-dimensional scheme of a wind tunnel with square section test chamber and low contraction ratio, N≈5.

It is clear that the new design is slightly longer and wider, but it is because of the influence of the test chamber´s width, as shown above.

Notice that in both cases corner 3 has the same shape as corner 4. Similarly, the entrance section of diffuser 4 is the same as of the power plant section, and using a diffuser semi-angle of 3,5°, this item is also well defined.

At this stage we have completely defined the wind tunnel centre line, so that we can calculate the length, L_{CL}, and width, W_{CL}, using:

$$L_{CL} = (L_{C1} - W_{EC1}/2) + L_{D1} + L_{TC} + L_{C} + L_{ST} + (L_{C4} - W_{ED5}/2)$$

$$W_{CL} = (W_{C4} - W_{EC4}/2) + L_{D5} + (W_{C3} - W_{ED4}/2).$$

The distance between the exit of the corner 1 and the centre of the corner 2, DC1_CC2, can be calculated through the expression (see Figure 11):

$$D_{C1\_CC2} = W_{CL} - W_{ED1}\left(r_{C1} + \frac{1}{2}\right).$$

On the other hand:

$$D_{C1\_CC2} = L_{D2} + [(W_{C2} - W_{EC2}/2)]$$

$$W_{EC2} = W_{ED2} \cdot e_{C2}$$

$$W_{C2} = W_{ED2} \cdot (r_{C2} + e_{C2})$$

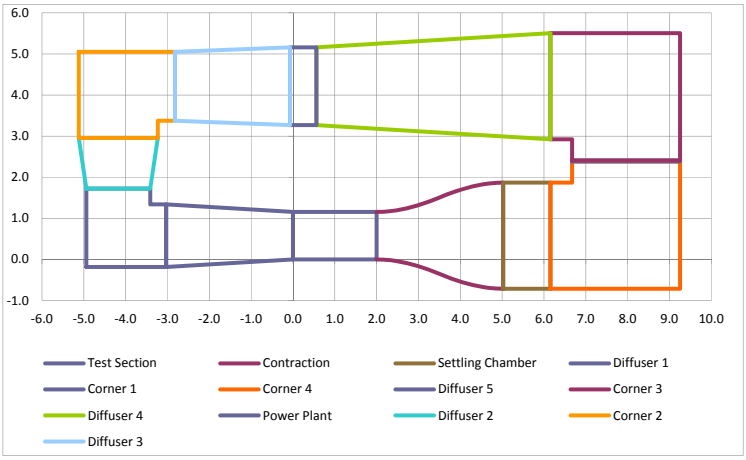

Figure 10. Non-dimensional scheme of a wind tunnel with rectangular section test chamber and low contraction ratio, N≈5.

$$W_{ED2} = W_{EC1} + 2 \cdot L_{D2} \cdot \tan(\alpha_{D2}/2).$$

Manipulating and combining those equations, we obtain:

$$L_{D2} = \frac{D_{C1\_CC2} - W_{EC1} \cdot (r_{C2} + e_{C2}/2)}{1 + 2 \cdot (r_{C2} + e_{C2}/2) \cdot \tan(\alpha_{D2}/2)}.$$

With this value, by substituting it into the previous expressions, we have all the parameters to design diffusers 2 and 3, and corner 2. Finally, it is necessary to check that the opening angles of diffuser 3 are below the limit. In case when the vertical opening angle, α, exceeds the limit, the best option is to increase the diffuser 1 length, if this is possible, because it improves flow quality and reduces pressure loss. If the wind tunnel length is in the limit, another option is to add the diffuser 5 to the original scheme. However, it will increase the overall width. When the limit of the horizontal opening angle, β, is exceeded, then the best option is to adjust the values of the expansion ratio in corners 1 and 2, because it will not change the overall dimensions.

The following case study is a wind tunnel with high contraction ratio, $N \approx 9$, and square section test chamber. In this case, the approximate area of the power plant section will be 2,000 x 2,000 m^2. In this case we have two compatible options to select the power plant. We can just select a matrix of 4 fans, 1,000 m diameter each. However, if the operating speed is rather high, in order to be able achieve the required pressure increment and the mass flow, we may need to use 1,250 m diameter fans. Figure 12 shows both options. Note that the overall planform is only slightly modified and the only difference is the position where the power plant is placed.

The design of the diffusers 2 and 3, and the corner 2 will be done following the same method as for the previous cases.

http://dx.doi.org/10.5772/54169

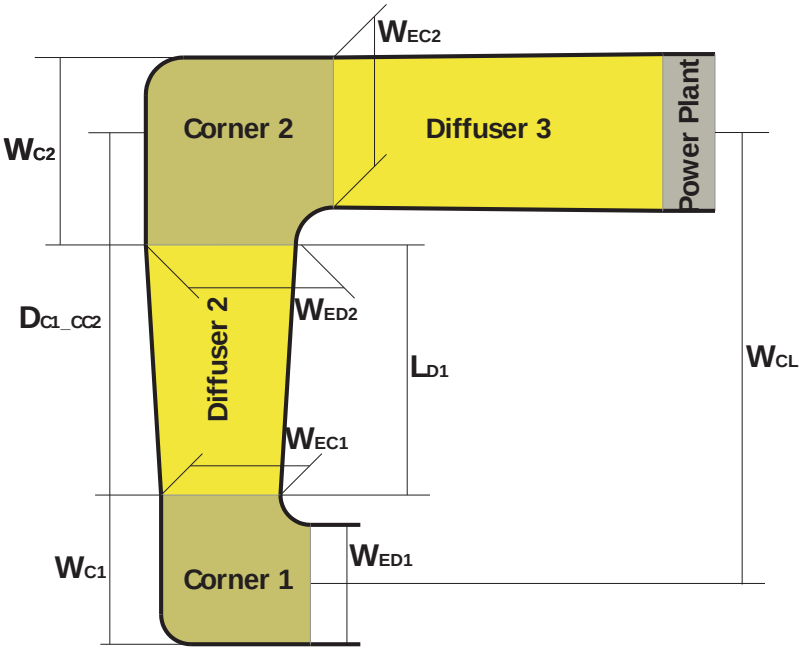

Figure 11. Scheme with the definition of the variable involving the design of diffuser 2 and 3, and corner 2.

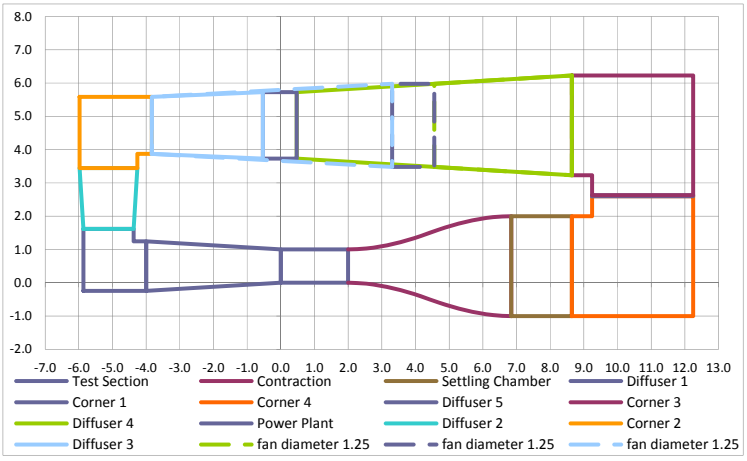

Figure 12. Non-dimensional scheme of a wind tunnel with square section test chamber and high contraction ratio, N≈9. Two different standard power plant options are presented.

5. Wind tunnel construction

One of the most important points mentioned in this chapter refers to the wind tunnel cost, intending to offer low cost design solutions. Up to now we have mentioned such modifications to the power plant, proposing a multi-fan solution instead of the traditional special purpose single fan.

The second and most important point is the wind tunnel's construction. The most common wind tunnels, including those with square or rectangular test sections, have rounded return circuits, like in the case of the NLR-LSWT. However, the return circuit of DNW wind tunnel is constructed with octagonal sections. Although the second solution is cheaper, in both cases different parts of the circuit needed to be built in factories far away from the wind tunnel location, resulting in very complicated transportation operation.

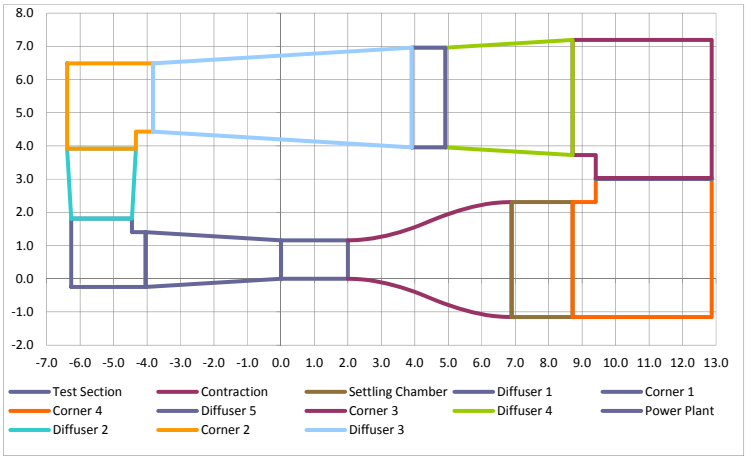

Figure 13. Non-dimensional scheme of a wind tunnel with rectangular section test chamber and large contraction ratio, N≈9.

To reduce the costs, all the walls can be constructed with flat panels, which can be made on site from wood, metal or even concrete, like in the case of ITER's wind tunnel. Figure 14 shows two wind tunnels built with wood panels and aluminium standard profile structure.

Both wind tunnels shown in Figure 14 are open circuit. The one on the left is located in the Technological Centre of the UPM in Getafe (Madrid) and its test chamber section is 1,20 x 1,00 m^2. Its main application is mainly research. The right one is located in the Airplane Laboratory of the Aeronautic School of the UPM. Its test chamber section is 0,80 x 1,20 m^2, and it is normally used for teaching purposes, although some research projects and students competitions were

http://dx.doi.org/10.5772/54169

done there as well. Despite the fact that these tunnels are open circuit, the construction solutions can be also applied to closed circuit ones.

Figure 14. Research and education purpose wind tunnels built with wood panel and standard metallic profiles, with multi-fan power plant.

According to our experience, the manpower cost to build a wind tunnel like those defined in figures 9 to 13 could be 3 man-months for the design and 16 man-months for the construction. With these data, the cost of the complete circuit, excluding power plant, would be about 70.000,00 €. In our opinion, the cost figure is very good, considering the fact that the complete building time possibly may not exceed even 9 months.

We have more reliable data with regard to the ITER wind tunnel, built in 2000-01. The whole cost of the wind tunnel, including power plant, work shop and control room, was 150.000,00 €.

This wind tunnel was almost completely built with concrete. Figure 15 shows different stages of the construction, starting from laying the foundations to the almost final view. The small photos show the contraction, with the template used for wall finishing, and the power plant.

6. Conclusions

A method for quick design of low speed and low cost wind tunnels, either for aeronautical and/or civil applications, has been presented.

The possibility of deciding between both applications means that the method allows achieving flow quality level as good as desired.

The method also allows to the designer to get a quick and rough estimation of the overall wind tunnel size, once the main design parameters are given.

The guidelines to choose the secondary design parameters are given as well.

To address the low cost of design and construction, the use of a multi fan power plant and rectangular duct sections is proposed as well.

Figure 15. Photographic sequence of the construction of the ITER Low Speed Wind Tunnel. The top left picture shows the foundations, the top right the contraction, the bottom left the power plant and the bottom right a view from the outside almost at the end of the construction.

Nomenclature

a_i, b_i, c_i, d_i	Family of polynomial coefficients of the contraction contour shape	
CFD	Computational Fluid Dynamics	
D_{C1_CC2}	Distance between the exit of the corner 1 and the centre of the corner 2	m
D_F	Unitary fan diameter	m
D_H	Studied duct section hydraulic diameter	m
e_i	Corner 'i' expansion ratio	
F_0	Area of the diffuser's narrow section	m^2
F_1	Area of the diffuser's wide section	m^2
H_{ent}	Section height of the duct´s entrance	m

http://dx.doi.org/10.5772/54169

H_{exit}	Section height of the duct´s exit	m
L	Studied duct length	m
L_i	Duct 'i' length	m
l_i	Duct 'i' non-dimensional length	
LSWT	Low Speed Wind Tunnel	
L_{WT}	Overall wind tunnel length	m
N	Contraction ratio	
n	Average number of corner vanes	
n_W, n_H	Dimensions of the fan matrix	
P	Power of the power plant	W
Q	Volumetric flow	m^3/s
r	Corner radius	m
Re	Reynolds number based on the hydraulic diameter	
r_i	Corner 'i' non-dimensional radius	
S	Diagonal dimension of the corner	m
t_1	Chord of the corner vane	m
V	Operating speed at the test chamber	m/s
V_{TC}	Maximum operating speed at the test chamber	m/s
W_{CL}, L_{CL}	Wind tunnel centre line width and length	m
W_{ent}	Section width of the duct´s entrance	m
W_{exit}	Section width of the duct´s exit	m
W_{ij}, H_{ij}	Duct j width and height of the i section (wide-end, $_W$; narrow-end, $_N$; constant,)	m
WTT	Wind Tunnel Tests	
$(x_N y_N)$	Narrow-end coordinates of the contraction contour shape	
$(x_W y_W)$	Wide-end coordinates of the contraction contour shape	
$\alpha_i/2$	Vertical contraction/opening semi-angle of the duct 'i'	deg
$\beta_i/2$	Horizontal contraction/opening semi-angle of the duct 'i'	deg
Δp	Pressure increment at the power plant section	Pa
ζ	Total pressure loss coefficient	
ζ_f	Friction pressure loss coefficient	
ζ_M	Singular pressure loss coefficient of a corner	
η	Fan efficiency	
λ	Friction coefficient per non-dimensional length of the studied duct	
ρ	Operating air density	kg/m^3

Acknowledgements

The authors would like to acknowledge to Instituto Tecnológico y de Energías Renovables (ITER) and to Grupo λ_3 of the UPM for their contribution.

Author details

Miguel A. González Hernández[1], Ana I. Moreno López[1], Artur A. Jarzabek[1], José M. Perales Perales[1], Yuliang Wu[2] and Sun Xiaoxiao[2]

1 Polytechnic University of Madrid, Spain

2 Beijing Institute of Technology, China

References

[1] Barlow, J. B, Rae, W. H, & Pope, A. Low-speed wind tunnel testing, John Wiley & Sons New York, (1999). rd ed.

[2] Borger, G. G. The optimization of wind tunnel contractions for the subsonic range, NASA Technical Translation / F-16899, NASA Washington, (1976).

[3] Eckert, W. T, Mort, K. W, & Jope, J. Aerodynamic design guidelines and computer program for estimation of subsonic wind tunnel performance, NASA technical note / D-8243, NASA Washington, (1976).

[4] Gorlin, S. M, & Slezinger, I. I. Wind tunnels and their instrumentation, Israel Program for Scientific Translations Jerusalem, (1966).

[5] Idel´Cik. I.E., Memento des pertes de charge: Coefficients de pertes de charge singulières et de pertes de charge par frottement, Eyrolles Editeur, Paris (1969).

[6] Maskell, E. C. A theory of the blockage effects on bluff bodies and stalled wings in a closed wind tunnel, R. & M. 3400, November, (1963).

[7] Mehta, R. D, & Bradshaw, P. Design Rules for Small Low-Speed Wind Tunnels, Aero. Journal (Royal Aeronautical Society), (1979). , 73, 443.

[8] Scheiman, J. Considerations for the installation of honeycomb and screens to reduce wind-tunnel turbulence, NASA Technical Memorandum / 81868, NASA Washington, (1981).

[9] The Royal Aeronautical Society. Wind tunnels and wind tunnel test techniques, Royal Aeronautical Society London, (1992).